Identification of the Primary Lesion of Toxic Aluminum in Plant Roots[1][OPEN]

Peter M. Kopittke*, Katie L. Moore[2], Enzo Lombi, Alessandra Gianoncelli, Brett J. Ferguson, F. Pax C. Blamey, Neal W. Menzies, Timothy M. Nicholson, Brigid A. McKenna, Peng Wang, Peter M. Gresshoff, George Kourousias, Richard I. Webb, Kathryn Green, and Alina Tollenaere

Schools of Agriculture and Food Sciences (P.M.K., B.J.F., F.P.C.B., N.W.M., B.A.M., P.W., P.M.G., A.T.) and Chemical Engineering (T.M.N.) and Centres for Integrative Legume Research (B.J.F., P.M.G., A.T.) and Microscopy and Microanalysis (R.I.W., K.G.), University of Queensland, St. Lucia, Queensland 4072, Australia; Department of Materials, University of Oxford, Oxford OX1 3PH, United Kingdom (K.L.M.); Centre for Environmental Risk Assessment and Remediation, University of South Australia, Mawson Lakes, South Australia 5095, Australia (E.L.); and TwinMic Beamline, Elettra-Sincrotrone Trieste, 34149 Trieste-Basovizza, Italy (A.G., G.K.)

Despite the rhizotoxicity of aluminum (Al) being identified over 100 years ago, there is still no consensus regarding the mechanisms whereby root elongation rate is initially reduced in the approximately 40% of arable soils worldwide that are acidic. We used high-resolution kinematic analyses, molecular biology, rheology, and advanced imaging techniques to examine soybean (*Glycine max*) roots exposed to Al. Using this multidisciplinary approach, we have conclusively shown that the primary lesion of Al is apoplastic. In particular, it was found that 75 μM Al reduced root growth after only 5 min (or 30 min at 30 μM Al), with Al being toxic by binding to the walls of outer cells, which directly inhibited their loosening in the elongation zone. An alteration in the biosynthesis and distribution of ethylene and auxin was a second, slower effect, causing both a transient decrease in the rate of cell elongation after 1.5 h but also a longer term gradual reduction in the length of the elongation zone. These findings show the importance of focusing on traits related to cell wall composition as well as mechanisms involved in wall loosening to overcome the deleterious effects of soluble Al.

Acid soils, in which soluble aluminum (Al) is elevated, comprise approximately 4 billion ha of the global ice-free land or approximately 40% of the world's total arable land (Eswaran et al., 1997). Although it has been known for over a century that Al decreases plant root growth, the underlying reasons for its toxic effects remain elusive. In a highly cited review of literature, Horst et al. (2010) stated that the "mechanism of Al-induced inhibition of root elongation is still not well understood, and it is a matter of debate whether the primary lesions of Al toxicity are apoplastic or symplastic." For example, in the symplast, Al has been reported to cause interference with DNA synthesis and mitosis, disrupt the function of the Golgi apparatus, damage membrane integrity, and inhibit mitochondrial functions. In the apoplast, Al may rigidify the cell wall (prevent loosening), inhibit cell wall enzymes, such as expansin, and cause cell rupturing (for review, see Rengel, 1997; Horst et al., 2010). The identification of numerous processes influenced by Al (such as those listed above) has occurred for a number of reasons. First, it is almost certain that Al does, indeed, have multiple mechanisms by which it reduces growth in both the short and long term. Second, there has been a lack of studies that have related the changes observed in these processes to the actual underlying changes in root elongation rate (RER). Thus, there typically has been no clear separation of the primary and secondary toxic effects of Al. Although some studies have examined the speed with which Al reduces RER, these studies have generally (1) been at comparatively coarse time steps and (2) not taken the additional step of relating these changes in RER to the underlying mechanism of toxicity (for example, see Llugany et al., 1995; Parker, 1995; Kidd et al., 2001; and Blamey et al., 2004).

In this study, we used kinematic analyses as the basis for elucidating the underlying mechanisms by which Al exerts toxic effects on the growth of soybean (*Glycine max*) roots. First, after exposure to Al, we captured digital images every 0.5 to 1 min so as to calculate

[1] This work was supported by the Australian Research Council (Future Fellowship nos. FT120100277 and FT100100337 to P.M.K. and E.L. and Discovery Early Career Researcher Award no. DE130100943 to P.W.), the Engineering and Physical Sciences Research Council (grant no. EP/I026584/1 to K.L.M.), and the International Synchrotron Access Program managed by the Australian Synchrotron and funded by the Australian Government (funding for travel to TwinMic Beamline at the Elettra Synchrotron Radiation Facility).

[2] Present address: School of Materials, University of Manchester, Manchester M13 9PL, UK.

* Address correspondence to p.kopittke@uq.edu.au.

The author responsible for distribution of materials integral to the findings presented in this article in accordance with the policy described in the Instructions for Authors (www.plantphysiol.org) is: Peter M. Kopittke (p.kopittke@uq.edu.au).

[OPEN] Articles can be viewed without a subscription.

www.plantphysiol.org/cgi/doi/10.1104/pp.114.253229

changes in overall RER with a resolution of 5 to 10 min. Second, we examined whether these changes in overall RER resulted from either or both (1) changes in the length of the root elongation zone (LEZ) or (2) changes in elemental elongation rate (EER), which is defined as the change in length per unit length of a small portion of tissue (Silk, 1992), as a measure of the rate at which individual cells elongate. Based upon these data, it seemed that Al is toxic by at least three separate but interrelated mechanisms. To provide additional information on these mechanisms, we: (1) used kinematic analyses to investigate the effects of aminoethoxyvinyl-Gly (AVG), an ethylene synthesis inhibitor; (2) examined changes in auxin distribution and movement in the root apex using a highly active synthetic auxin-response element (referred to as DR5) with a minimal promoter-GUS reporter gene (DR5::GUS); (3) investigated rapid changes in the mechanical properties of root cell walls using creep analysis; and (4) used synchrotron-based low-energy x-ray fluorescence spectromicroscopy (LEXRF) and high-resolution secondary ion mass spectroscopy (NanoSIMS) to examine the spatial distribution of Al on cellular and subcellular levels in roots exposed to Al for only 30 min. This integrated approach has allowed us to identify the sequence of processes whereby Al reduces the growth of soybean roots in the short term.

RESULTS

Magnitude and Symptoms of Al Toxicity

A concentration of 10 μM Al in solution culture reduced soybean 'Bunya' RER over 48 h by 54%, with a 76% reduction at 30 μM Al and a 90% reduction at 75 μM Al (Supplemental Fig. S1A). These three Al concentrations, which are similar to concentrations of Al

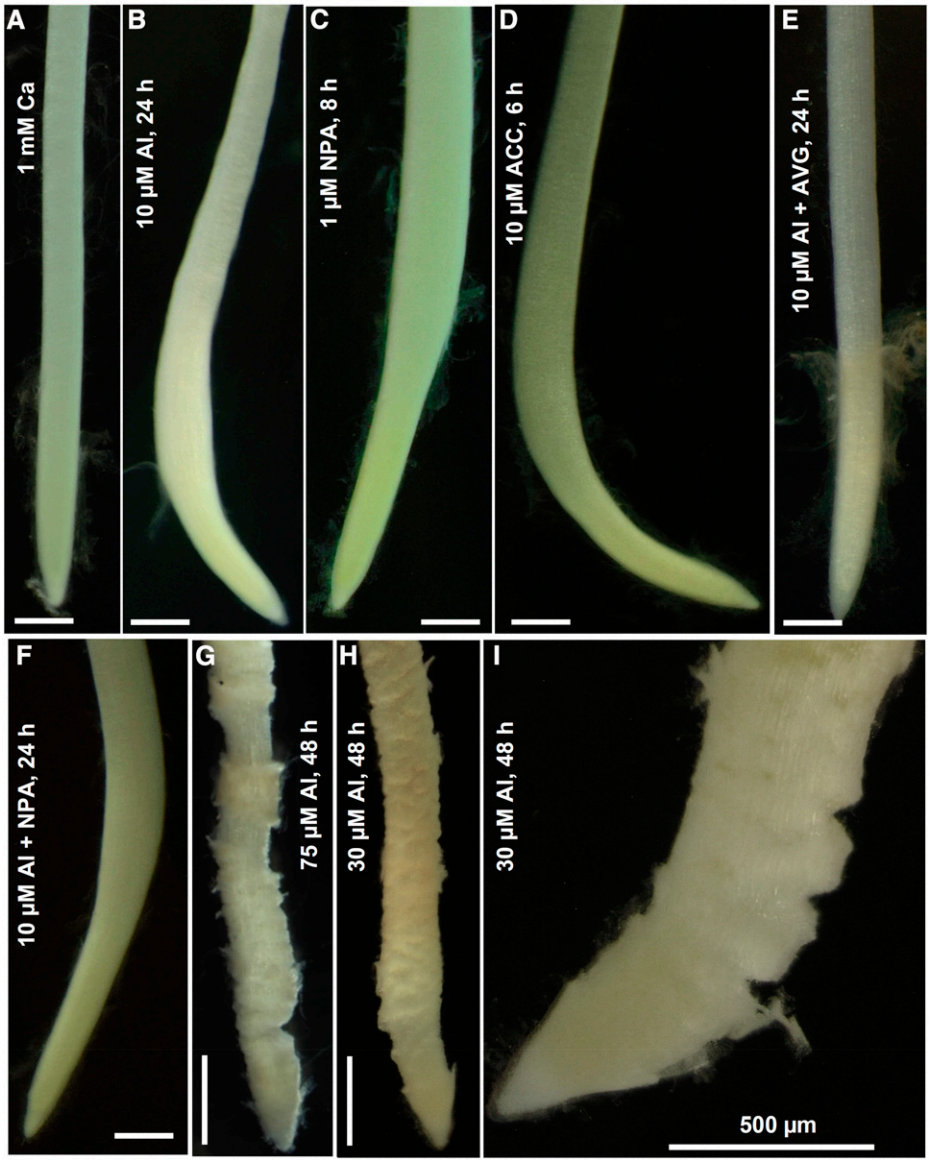

Figure 1. Light micrographs of soybean root tips. Roots were exposed to Ca (A), 10 μM Al (B), napthylphthalamic acid (NPA; C), 1-aminocyclopropane-1-carboxylic acid (ACC; D), Al plus AVG (E), Al plus NPA (F), 75 μM Al (G), or 30 μM Al (H and I) for the periods indicated. Bars in A to H = 1 mm.

often found in acidic soils (Menzies et al., 1994), formed the focus of this study.

Other than effects on RER, this initial experiment showed that there were two distinct symptoms of Al toxicity: (1) radial swelling behind the apex (Fig. 1, A and B) and (2) rupturing of the rhizodermis and outer cortex (Fig. 1, A and G–I). The radial swelling was most pronounced at 10 μM Al, decreasing in severity and frequency with increasing Al (Fig. 1; Supplemental Table S1; Supplemental Movie S1). Radial swelling has been observed in roots exposed to soluble Al (Sasaki et al., 1997; Zelinová et al., 2011), and we noted a similarity to the symptom defined as thick root syndrome that sometimes occurs in greenhouses (Pierik et al., 1999). This symptom has been ascribed to the effects of hormones, specifically ethylene or auxin, which increase radial expansion (Alarcon et al., 2013). Indeed, we found that 10 μM Al resulted in root swelling similar to that caused by the addition of either 1 μM NPA (an auxin transport inhibitor) or 10 μM ACC (an ethylene precursor; Fig. 1; Supplemental Table S1), and that roots often did not swell after the addition of AVG to solutions containing 10 μM Al (Fig. 1E). Interestingly, the addition of 4 μM AVG (an ethylene synthesis inhibitor) partially alleviated the toxic effects of 30 μM Al on root growth, with average RER in the period from 0 to 4 h after exposure being 0.67 mm h^{-1} at 30 μM Al but 1.3 mm h^{-1} at 30 μM Al + AVG (Supplemental Fig. S1B). In contrast to radial swelling, there was no rupturing of the outer tissues at 10 μM Al, but ruptures increased in severity with ≥30 μM Al (Fig. 1; Supplemental Table S1). The formation of ruptures caused by soluble Al has been the

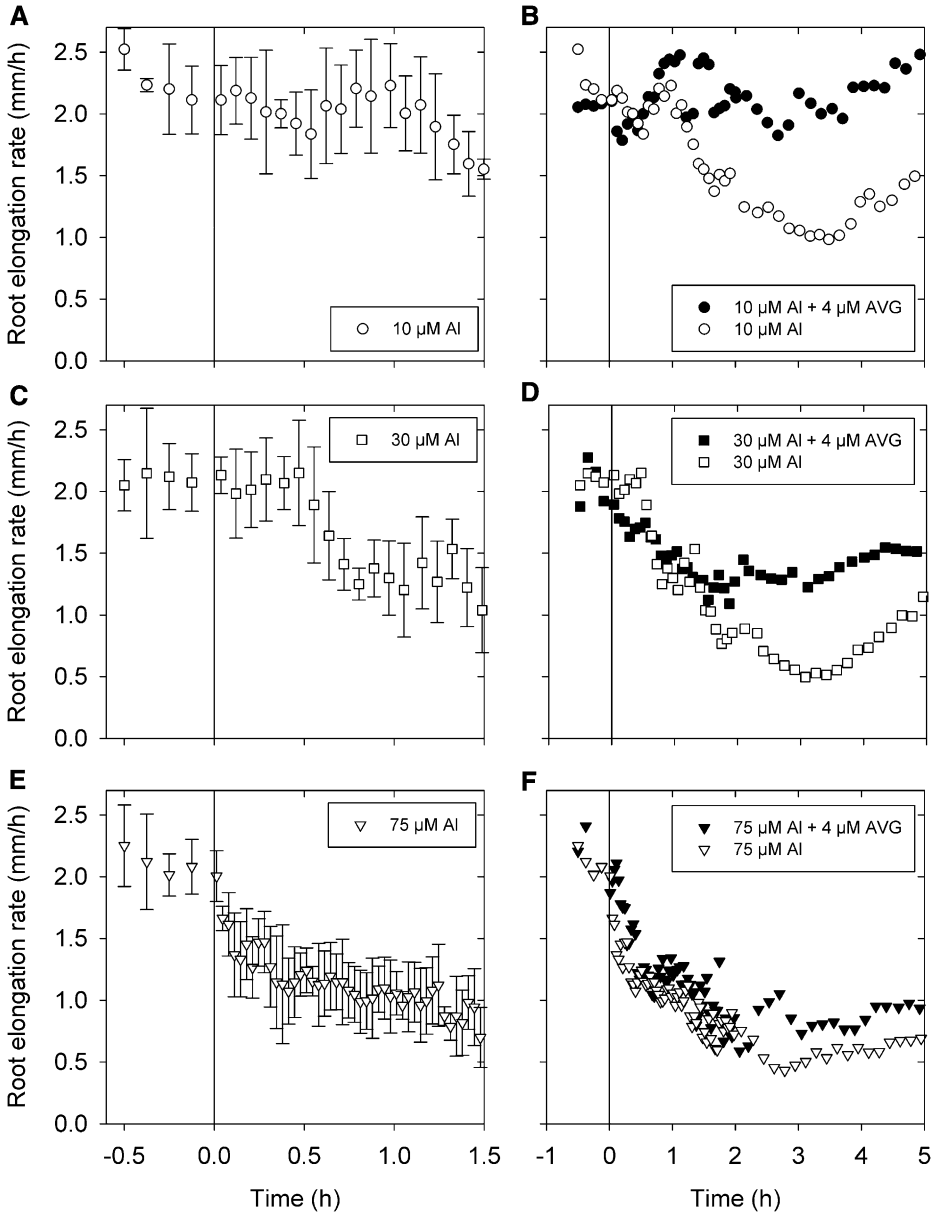

Figure 2. RER in soybean seedlings exposed to 10, 30, or 75 μM Al with or without AVG. Data are presented for the first 2 h after exposure (A, C, and E) and the entire 12-h period (B, D, and F). The SD for each time (five replicates) is shown in A, C, and E but, for clarity, not in B, D, or F. The vertical line represents the time at which the roots were exposed to Al. For the controls, RER was constant across the experimental period (as shown here in the pretreatment phase).

subject of much investigation (Yamamoto et al., 2001), and it has been ascribed to an inability of the walls of the outer tissues of the root elongation zone to loosen as required for anisotropic cell growth (Kopittke et al., 2014). The ruptures were observed to form in the elongation zone (Supplemental Movie S2).

Kinetics and Mechanisms of Al-Induced Reductions in Root Growth

Kinematic analyses of approximately 25,200 images using KineRoot (Basu et al., 2007) showed that soluble Al rapidly exerts its toxic effects in decreasing RER, with less time taken for root growth to decrease at higher Al in solution (Fig. 2, A, C, and E). For example, 10 μM Al reduced RER by 25% after 90 min, 30 μM Al reduced RER by 25% after 30 min, and 75 μM Al reduced RER by 25% after 5 min. Soluble Al decreased RER further over the next 1.5 h followed by a recovery period of approximately 2 h (Fig. 2, B, D, and F). This was more evident at 10 and 30 μM Al than at 75 μM Al. The presence of 4 μM AVG in solutions containing Al had the effect of almost eliminating the transient toxic effect of 10 μM Al from 1.5 to 3 h (Fig. 2B) and reducing that of 30 μM Al (Fig. 2D). In contrast, AVG had only a minor effect on the severely toxic effect of 75 μM Al on RER (Fig. 2F).

We divided the toxic effects of Al over the entire 12-h exposure period into three phases based upon changes in RER. The first phase from 0 to 1.5 h (Fig. 2) was defined as the initial reduction in RER that was not influenced by the addition of AVG (Figs. 2 and 3). There was no effect of 10 μM Al in this phase, but 30 and 75 μM Al had substantial toxic effects. The approximately 50% to 60% reduction in RER was caused mainly by a decrease in the maximum elemental elongation rate (MEER) with little decrease in the LEZ (Fig. 3; Supplemental Fig. S2–S4). For example, in solutions containing 30 μM Al, MEER decreased from 31% per hour in the basal solutions to 18% per hour after 1.5 h, whereas LEZ only decreased slightly (from 6.9 to 6.4 mm).

The second phase of root growth in Al solutions from 1.5 to 5 h was characterized by a temporary decrease in RER from 1.5 to 3 h followed by an increase in RER over the next 2 h to the level observed at the beginning of this phase (Figs. 2, B, D, and F and 3). Importantly, the reduction in RER by 10 and 30 μM Al within this second phase was entirely alleviated by the addition of AVG (Figs. 2, B and D and 3). Addition of

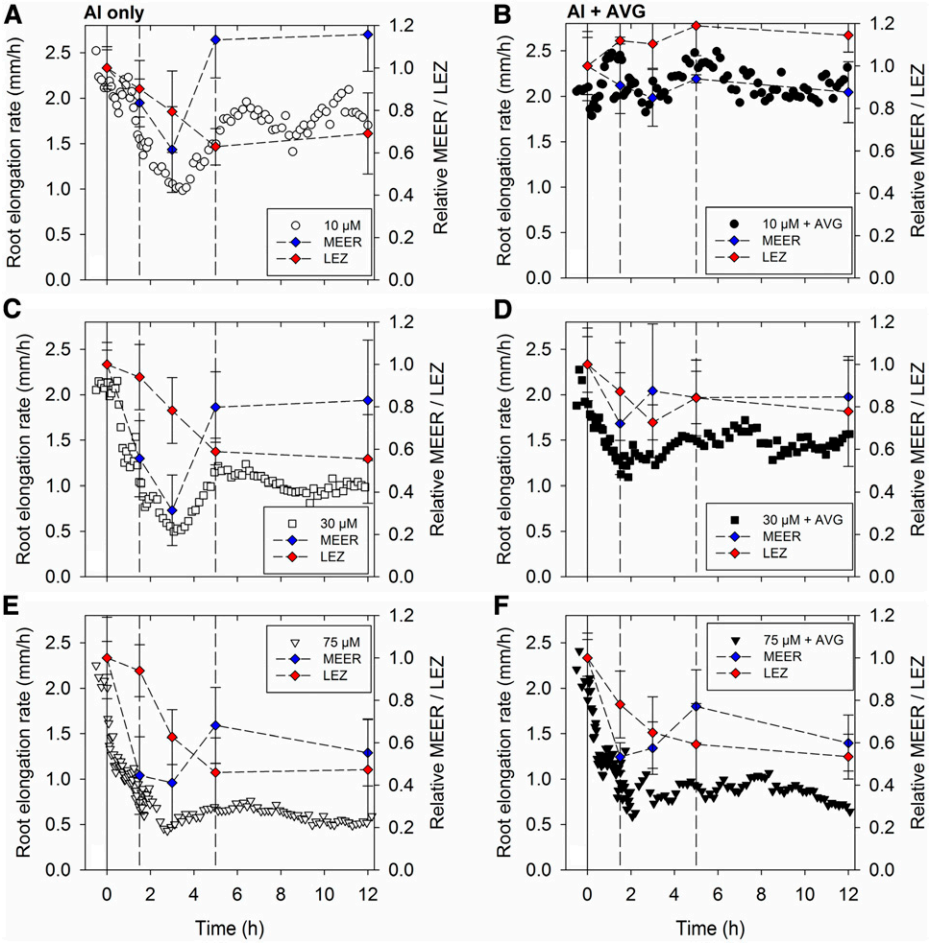

Figure 3. RER in soybean seedlings exposed to 10, 30, or 75 μM Al either without (A, C, and E) or with (B, D, and F) AVG. For clarity, the SDS (five replicates) are not shown for RER (Fig. 2). The dashed vertical lines are at times of 1.5 and 5 h, corresponding to different patterns of growth. The MEER (Supplemental Fig. S4) and the LEZ (Supplemental Figs. S2 and S3) have been plotted to help explain the changes in RER.

AVG, an ethylene inhibitor, indicates a role of ethylene in this phase, which started 1.5 h after exposing roots to Al. In further contrast to the first phase, in which AVG did not modify the severe toxicity of 30 and 75 μM Al, the alleviating effect of AVG on RER during the second phase was most evident at 10 and 30 μM Al (Figs. 2, B, D, and F and 3). Within this second phase, the reduction in RER was caused primarily by a further decrease in the MEER and to a lesser extent, a decrease in LEZ (Fig. 3; Supplemental Figs. S2–S4). Interestingly, the subsequent increase in RER from 3 to 5 h was caused by a recovery in MEER (Fig. 3; Supplemental Fig. S4).

During the third phase of growth (5–12 h), it seemed that RER at 10 μM Al continued to increase slightly for 2 h (Fig. 3A), but this period was characterized overall by RER decreasing slightly but not significantly at all Al levels (Fig. 3, A, C, and E). Within this period, the deleterious effects of Al could be alleviated partially by the addition of AVG (Fig. 3). Al-induced growth reduction within this final phase was primarily caused by a low LEZ at 10 and 30 μM Al; MEER also decreased slightly at 75 μM Al (Fig. 3; Supplemental Figs. S2–S4).

Upon exposure to 30 μM Al, the bulk Al concentration in the apical root tissues (0–10 mm) increased rapidly from 2.8 to 38 $\mu g\ g^{-1}$ (fresh mass basis) in the first phase (0–1.5 h) before increasing to 220 $\mu g\ g^{-1}$ at the end of the third phase (12 h; Supplemental Table S2). The initial increase in Al was most rapid in the meristematic and transition zones (0–3 mm from the apex), where the Al concentration increased 18-fold from the 0- to 1.5-h exposure periods (Supplemental Table S2).

Spatial Distribution of Al in Roots

The speed with which Al exerts its toxic effects on root growth (Figs. 2 and 3), swelling (Supplemental Table S1), and rupturing (Fig. 1; Supplemental Table S1) suggested that it would be useful to examine the spatial distribution of Al within the root cylinder at 0.75, 2, and 6 mm from the apex. Therefore, roots were exposed to 30 μM Al for 0.5 h, a time approximately before the start of the rapid decrease in RER (Fig. 2C). (Roots were exposed to 30 μM Al for 24 h as well to evaluate Al distribution in the long term.) The cellular distribution of Al using both LEXRF and NanoSIMS revealed that most Al was located in the outer cellular layers within 0.5 h, with a marked radial decrease inward at all three distances from the apex (Fig. 4). It is noteworthy that, even after exposing roots to 30 μM Al for 24 h, LEXRF imaging showed that the majority of Al was located in the outer cellular layers (Fig. 5).

Subcellular examination after 0.5 h of exposure revealed details on the Al, which accumulated toward the outside of the root at 0.75, 2, and 6 mm from the apex (Fig. 4, A–C). With increasing distance from the apex, Al was bound strongly by mucigel on the root surface, walls of the border cells, and walls of the rhizodermal cells (Fig. 4). Importantly, it is in the elongation zone, typified by the sections 6 mm from the apex, where Al initially reduces cell elongation (Supplemental Figs. S3–S6) and swelling and rupturing occur (Supplemental Figs. S3–S6). It is also important to note that the Al present in the outer cells and those further into the root cylinder was bound mostly within the cell wall. Indeed, Al was located especially in the junctions between cells (Fig. 4D), which are filled with pectin-rich polysaccharides (Carpita and McCann, 2000) with a low degree of

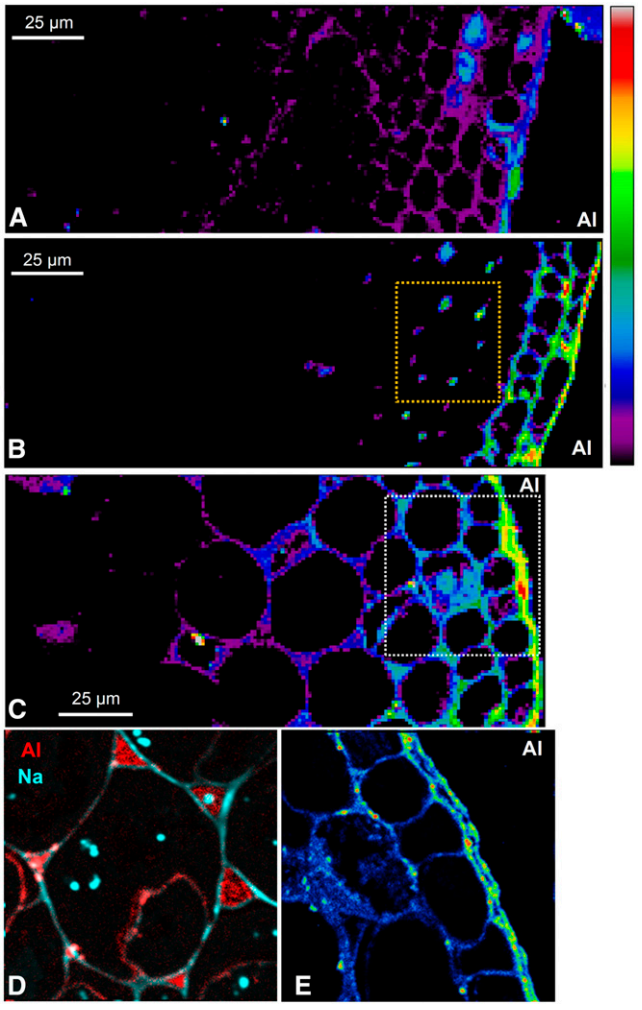

Figure 4. Distribution of Al using LEXRF in a 7-μm-thick transverse section of a soybean root exposed to 30 μM Al for 0.5 h at a distance of 0.75 (A), 2 (B), or 6 (C) mm from the apex, with the exterior of the root toward the right. The higher magnification NanoSIMS image in D is of a similar region (indicated by the yellow dotted box in B) but from a subsequent transverse section, and the NanoSIMS image in E is of a similar region (indicated by the white dotted box in C). For all images other than D, the signal intensity is presented as a color scale, with brighter colors indicating higher concentration; relative intensities are comparable within each image only. In D, color intensities are related to concentrations of Al and sodium. In A to C, a logarithmic scale is used to represent the colors to more clearly show the distribution of the lower concentrations of Al in the inner tissues (Fig. 5 shows a comparison of linear and logarithmic scales).

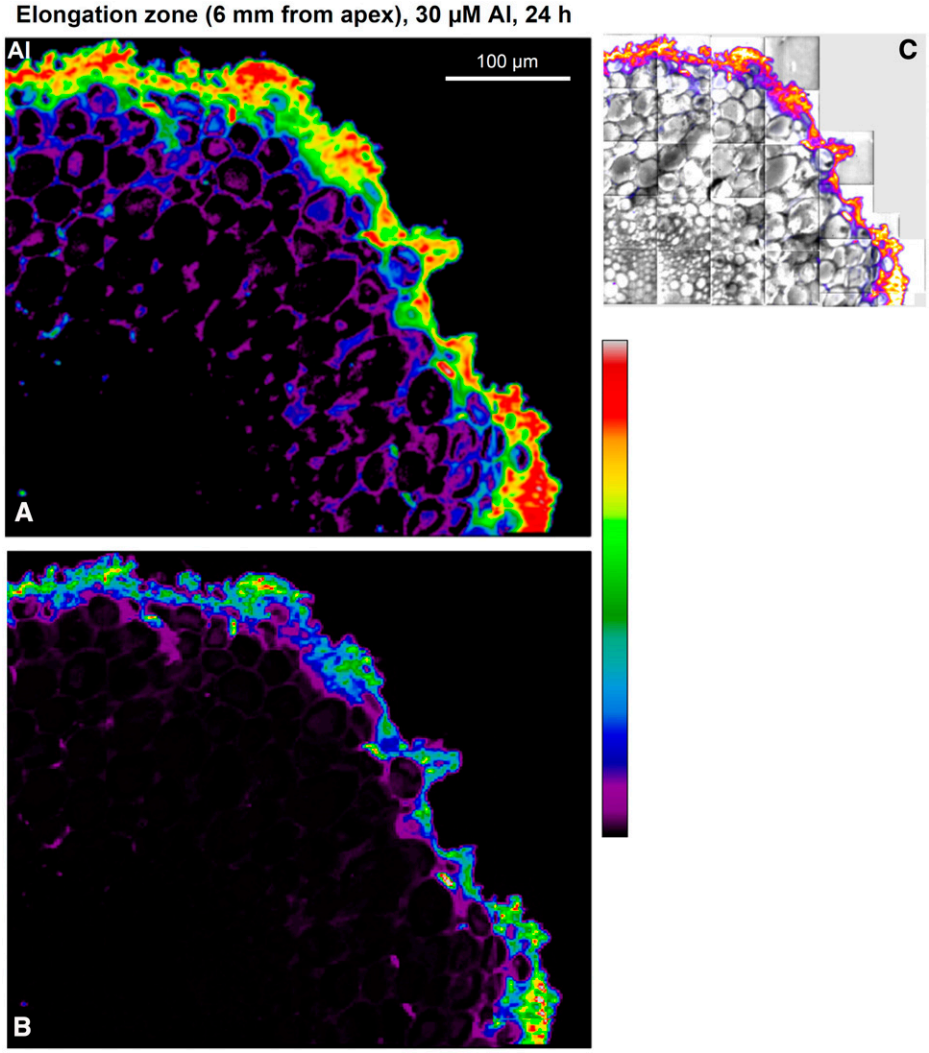

Figure 5. Distribution of Al using LEXRF in a 7-μm-thick transverse section of a soybean root 6 mm from the apex (i.e. elongation zone) after exposure to 30 μM Al for 24 h. The signal intensity is shown as a color scale, with brighter colors indicating higher concentration. Both A and B show the distribution of Al, but a logarithmic scale is used to represent the colors in A to more clearly show the distribution of the lower concentrations of Al in the inner tissues. In B, a linear scale is used to represent the colors. For C, the map for Al is overlaid with the map for absorption. Note that the root has ruptured; hence, the rhizodermis and outer cortex are torn.

methylesterificiation (i.e. high negative charge; Guillemin et al., 2005). This is in keeping with the contention that Al bound strongly in the cell wall limits cell elongation and root growth (Ma et al., 2004).

Mechanical Properties of Cell Walls

In keeping with Al distribution, exposure of roots to 30 μM Al resulted in a decrease in the ability of the cell walls to loosen as required for elongation, with grouped regression analysis indicating significant differences between treatments ($P < 0.001$; Fig. 6). Indeed, exposure to Al for 0.5 h reduced strain (elongation under tension), on average, from 4.5% to 4.0%; corresponding values for 1 and 3 h were 2.6% and 1.8%, respectively. The magnitude of this Al-induced inhibition of wall loosening is similar to that of previous studies (Ma et al., 2004; Jones et al., 2006) on the effects of Al after exposure for 3 to 9 h. By using shorter periods of exposure, we were able to relate cell wall strength to overall changes in RER and MEER. Indeed, these reductions in strain (Fig. 6) correspond approximately to the reductions in RER and MEER after the exposure of roots to 30 μM Al for up to 3 h (Figs. 2 and 3).

The Roles of Ethylene and Auxin

The roles of ethylene and auxin in decreased root growth when exposed to Al have been suggested previously (Sun et al., 2010). We had also noted the presence of radial swellings that formed behind the apex in roots exposed to Al (Fig. 1) and the partial alleviation in RER upon the addition of AVG (an ethylene synthesis inhibitor; Figs. 2 and 3). A construct containing the GUS reporter gene driven by a minimal promoter and the auxin-response element, DR5, was used to determine how Al influences the spatial distribution of auxin in the root. In the absence of added Al (control), GUS was primarily expressed in the columella of the root cap (Fig. 7, A and B), this being consistent with results of similar studies (for example, Sun et al., 2010 in Arabidopsis [*Arabidopsis thaliana*]

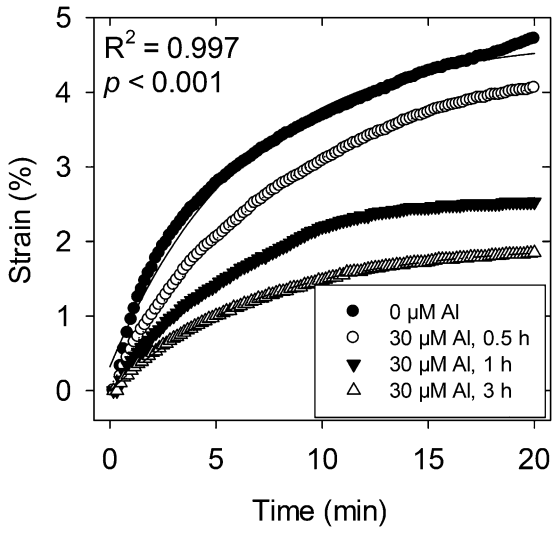

Figure 6. Extension of cell walls in the elongation zone of soybean roots grown in solutions containing 30 μM Al for 0.5, 1, or 3 h compared with those grown in basal solution (control). Grouped regression analysis indicated significant differences between curves ($P < 0.001$). Each value is the arithmetic mean of three replicates.

and Turner et al., 2013 in soybean). The addition of Al to the nutrient solution had two notable effects. For the first effect, the expression of GUS increased greatly in the lateral root cap and the rhizodermis to a lesser extent (Fig. 7, D–M). Increased expression of GUS in the apex was evident within 0.5 h at 10, 30, and 75 μM but generally greatest at 75 μM (Fig. 7, J–M). Interestingly, the addition of AVG at 30 μM Al reduced changes in GUS expression in the apex, especially 0.5 h after exposure to Al (Fig. 7, F–H). A second effect caused by the addition of Al was observed in the more proximal tissues. Specifically, tissues ≥10 to 20 mm from the apex in roots exposed to 0 μM Al (control) had increased expression of GUS, which gradually strengthened with increasing distance (Fig. 7A; Supplemental Fig. S5A). In contrast, the proximal expression of GUS in Al-exposed roots was evident closer to the apex, often at a distance of only approximately 5 to 10 mm, which was illustrated for roots at 75 μM Al (Supplemental Fig. S5B). Additional microscopic examination showed that this increased GUS expression in tissues closer to the apex was associated with the formation of lateral roots (Supplemental Fig. S5, C–G). Indeed, increased root branching and the formation of lateral roots close to the apex (i.e. loss of apical dominance) are common symptoms of Al toxicity (Kopittke et al., 2008 and refs. therein).

DISCUSSION

Here, we have shown that the first toxic effect (lesion) of Al is apoplastic, with Al directly reducing individual cell elongation (i.e. a decrease in MEER). Indeed, an increase in Al concentration from 10 to 75 μM reduced the time for measurable effects (Fig. 2, A, C, and E) from 90 to 5 min. This first toxic effect of Al is attributed to a direct inhibition of anisotropic cell expansion in the elongation zone resulting from the strong binding of Al to the cell wall and a prevention of wall loosening (Jones et al., 2006; Kopittke et al., 2008, 2014; Rangel et al., 2009). As explained by Winship et al. (2010), the energy for cell growth derives from turgor (which remains constant) coupled with a loosening of the cell wall.

This conclusion regarding the importance of Al binding to the cell wall is based upon several observations. First, the decrease in RER was caused by

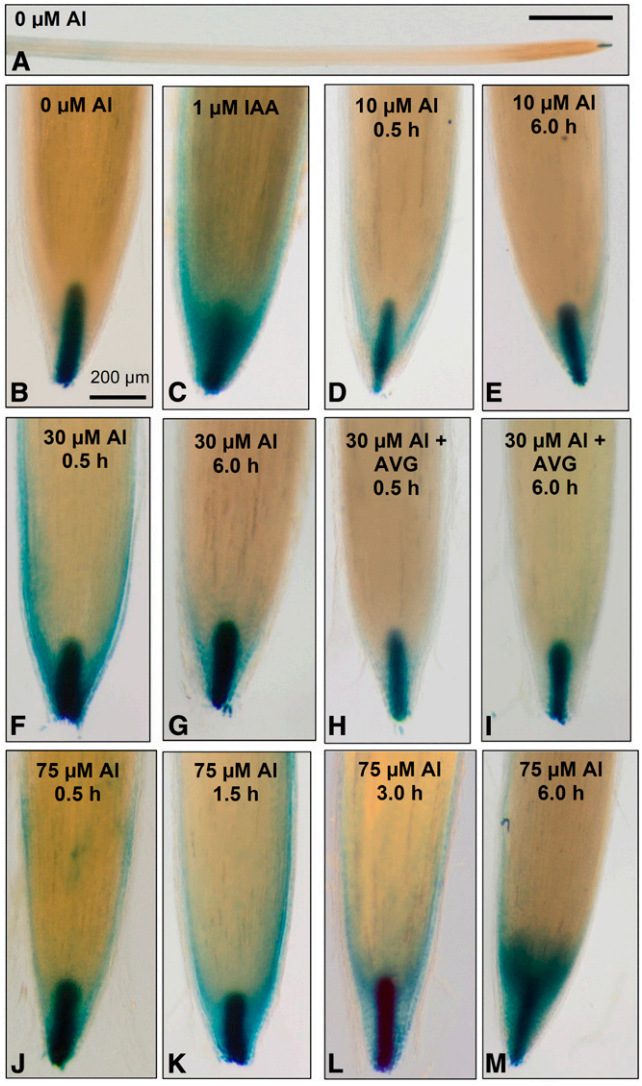

Figure 7. Expression of the GUS reporter gene fused to a minimal promoter and the DR5 auxin-responsive promoter element (DR5::GUS) in control roots (A and B) and after exposure to indole-3-acetic acid (IAA; C) or 10 (D and E), 30 (F–I), or 75 (J–M) μM Al for up to 6 h. The ethylene synthesis inhibitor, AVG, was also added to some solutions containing 30 μM Al (H and I). An overview of a root grown in a control solution (1 mM Ca and 5 μM B at pH 4.8) is presented in A, with B to M showing only the root apical tissues.

a reduction in MEER but not LEZ (Fig. 3); responses in which the elemental expansion rate changes while the growth zone length stays constant are known to reflect a direct influence at the level of the expansion mechanism (Baskin, 2013). Second, creep analysis (Fig. 6) showed that exposure to Al rapidly reduces the ability of cell walls to loosen in the elongation zone as required for elongation. This is in general agreement with timing of reductions in RER and MEER (Fig. 6). Third, using synchrotron-based LEXRF and NanoSIMS, we have shown that, after only 0.5 h of exposure to 30 μM Al, the majority of the Al accumulates within the cell walls of the outer tissues (Fig. 3). This is especially pertinent regarding the cells of the elongation zone (Fig. 4, C and E), which undergo rapid anisotropic growth. Fourth, the direct inhibition of cell elongation evident at higher concentrations of Al (Figs. 2, A, C, and E and 3; Supplemental Figs. S2–S4) corresponds to the treatments where ruptures occur through continued growth of inner tissues (Kopittke et al., 2014).

We have shown that a second effect of Al is that it alters the biosynthesis and distribution of ethylene and auxin, causing both a transient decrease in the rate of cell elongation (MEER) approximately 1.5 to 5 h after exposure and also, a longer term partial reduction in LEZ (Fig. 3; Supplemental Figs. S3 and S4). Ethylene is known to positively control auxin biosynthesis in the root apex (Swarup et al., 2007), with auxin transported basipetally through the rhizodermis (Fig. 7). In this study, the importance of this interaction between ethylene and auxin in influencing the growth of Al-exposed roots is evidenced by: (1) the formation of radial swellings behind the apex in Al-exposed roots, which are markedly similar to those caused by ACC and NPA (Fig. 1); (2) the almost complete alleviation by AVG of the Al-induced decrease in RER in phase 2 (Figs. 2 and 3; Supplemental Figs. S2–S4); (3) increased accumulation of auxin at the root apex (increased expression of GUS controlled by the auxin-responsive element DR5; Fig. 7; Supplemental Fig. S5), which may be indicative of an increase in auxin biosynthesis and/or an alteration in basipetal auxin transport (Kollmeier et al., 2000);and (4) the decrease in GUS expression when AVG is included in solutions containing 30 μM Al (Fig. 7). The addition of AVG to solutions containing Al reduced the expression of GUS (although it did not prevent rupturing; Supplemental Fig. S6), suggesting that Al promotes the production of ethylene, which then induces a change in auxin distribution (Sun et al., 2010). It is not clear, however, why Al alters the biosynthesis and distribution of these two important hormones in roots. It is possible that Al directly causes the biosynthesis of ethylene or that this stress hormone is synthesized in response to increased cell wall rigidity or subsequent rupturing. In this regard, however, it is noteworthy that a reduction in wall loosening, which is evident by a reduction in MEER that reduces RER by 25% after approximately 5 min at 75 μM Al, precedes alterations in auxin as shown using the auxin-responsive DR5::GUS reporter construct (Fig. 7). These subsequent changes in auxin expression and associated cell wall acidification (Cosgrove, 1993) suggest a response to Al-induced rigidity of the walls of outer cells in the root elongation zone. However, additional studies are required to investigate why biosynthesis of ethylene increases in Al-toxic solutions.

In conclusion, we have shown that the toxic effects of Al were rapid, reducing the elongation of soybean roots within 5 min at 75 μM Al. This initial toxic effect was caused by a direct inhibition of cell elongation because of the binding of Al to the cell walls of the rhizodermis and outer cortex and an inhibition of loosening as required as part of the elongation processes. In addition to this direct inhibition of cell elongation, Al also altered ethylene and auxin biosynthesis and accumulation, which after approximately 1.5 h, resulted in both a transient decrease in the rate of cell elongation (MEER) and also, a longer term gradual reduction in LEZ. For the first time to our knowledge, changes in root functioning have been related to high-resolution kinematic analyses of root growth with complementary use of molecular biology, rheology, and advanced imaging techniques. This has provided critical information required for the breeding and selection of Al-resistant plants to increase productivity in the 40% of worldwide arable soils that are acidic. In particular, we have shown here the importance of focusing on traits related to cell wall composition as well as traits involved in wall loosening—these being important for overcoming the deleterious effects of Al.

MATERIALS AND METHODS

Symptoms and Magnitude of Al Toxic Effects

An initial solution culture experiment conducted as described by Kopittke et al. (2008) determined the rhizotoxic effects of soluble Al on 2-d-old soybean (*Glycine max* 'Bunya') seedlings. These were transplanted into a Perspex strip on top of a glass beaker containing 650 mL of continuously aerated basal solution (1 mM $CaCl_2$ and 5 μM H_3BO_3) at pH 4.7. Individual treatments were imposed after 24 h by transferring the seedlings to new beakers, which contained 1 mM $CaCl_2$, 5 μM H_3BO_3, and 0, 10, 30, 50, 75, or 100 μM $AlCl_3$. In all cases, the treatment solution was decreased to pH 4.7 by adding 0.1 M HCl, the volume of which varied depending upon the Al concentration. The speciation of Al in these simple nutrient solutions was modeled using PhreeqcI; Al^{3+} was the dominant Al species at pH 4.7 (Supplemental Table S3).

This experiment was conducted to establish a dose-response curve using a digital camera (Kopittke et al., 2008), which allows accurate measurement of changes in RER over intervals of approximately 4 h. Furthermore, light microscopy was used to determine the nature and timing of any symptoms of Al rhizotoxicity.

Kinematic Analyses

This experiment aimed to refine the assessment of Al effects on RER over 5- to 10-min intervals for 12 h after exposure to Al and determine the extent to which changes in RER arise from changes in EER and LEZ. This experiment also examined the effects of AVG, an ethylene synthesis inhibitor, given that some of the symptoms of Al rhizotoxicity observed in the previous experiment appeared similar to those caused by ethylene and indole-3-acetic acid .

A stereo microscope (Olympus SZX16) with a 10-megapixel camera (Olympus SC100) was placed horizontally to capture images of roots growing vertically. After 24 h in basal solutions as detailed above, the Perspex strip was removed from the beaker and briefly dipped into 1 mM $CaCl_2$ (pH 4.8) solution with suspended activated carbon particles (242276; Sigma Aldrich) so as to track

elongation at various points along the root. The strip was then returned to the basal solution, and 60 images were captured at 0.5-min intervals to determine RER, EER, and LEZ under nonlimiting conditions. The beaker was then removed, and the Perspex strip was placed into another beaker containing 1 mM calcium, 5 μM B, and Al at pH 4.8. Images were captured for the next 12 h at 0.5-min intervals for the first 120 min and 1-min intervals for the remaining 600 min. It was less than 1 min from the time that the seedling was placed in the treatment solution to when the first image was captured. The root was again briefly dipped in the solution containing activated carbon every 4 h to ensure sufficient particles in the elongation zone. Roots were examined in a total of six treatments: three concentrations of Al (10, 30, and 75 μM) corresponding to a reduction in RER of 50%, 75%, and 90%, respectively, after 48 h of exposure (Supplemental Fig. S1) each at 0 or 4 μM AVG. A preliminary study identified that AVG could be added at the same time as Al. Five replicate seedlings per treatment were examined per week because only one seedling could be examined at a time.

The 30 roots yielded approximately 25,200 images, which were processed using KineRoot (Basu et al., 2007). After these analyses, the data from the images were averaged to determine changes in RER over 5-min intervals (10 or 30 μM Al) or 2-min intervals (75 μM Al) for the first 2 h and then 10-min intervals for the remaining 10 h. Using the growth velocity profiles (Silk, 1992) calculated by KineRoot, Equation 1 was fitted using Systat v13.1 (Cranes Software):

$$V = b\left(1 - 1\Big/\exp\left((cD)^h\right)\right) \quad (1)$$

where V is the growth velocity at any given distance from the apex (millimeters per hour), b is the maximum growth velocity along the root (millimeters per hour), c is a strength coefficient, D is the distance from the root apex (millimeters), and h is a shape coefficient (Kinraide, 1999). The EER was then calculated as the derivative of Equation 1, and the LEZ was determined using the relative velocity profile defined as the region in which 80% of root elongation occurs (i.e. between 10% and 90% of the relative velocity profile).

Spatial Distribution of Al in Root Tissues

The rapidity with which Al exerts its toxic effect on root elongation suggested that it would be useful to determine the location of Al in the root tip. The use of dyes, such as morin, has provided valuable information regarding the movement of Al in roots, but Eticha et al. (2005) showed that dyes are not necessarily able to detect all Al bound within the cell wall given the strength of its binding. To overcome this drawback, the LEXRF facility at the TwinMic Beamline at the Elettra Synchrotron Radiation Facility (Kaulich et al., 2006) and NanoSIMS were used to assess Al distribution in the root tip.

Soybean seedlings were grown for 24 h in basal solutions (1 mM $CaCl_2$ and 5 μM H_3BO_3) at pH 4.7 and transferred to solutions containing 1 mM $CaCl_2$, 5 μM H_3BO_3, and 30 μM Al (pH 4.7) for 0.5 or 24 h. The seedlings were rinsed briefly in 1 mM $CaCl_2$ (pH 4.7), and three 200-μm transverse sections were cut from the roots 0.75, 2.0, and 6 mm from the apex. The sections were placed in planchettes that were 275 μm deep, filled with hexadecane, and frozen in a Bal-Tec HPM010 High-Pressure Freezer. The planchettes were split apart and stored under liquid nitrogen before freeze substitution (Leica EM AFS2) in 2% (v/v) glutaraldehyde in acetone at −90°C for 48 h, warming to 20°C, washing in ethanol, infiltration with LR White Resin, and polymerization. After storage at ambient temperature, a Reichert Ultracut Microtome was used to cut 7-μm-thick sections, which were placed on 4-μm Ultralene Film.

The LEXRF measurements were conducted using the TwinMic Beamline at the Elettra Synchrotron Radiation Facility (BL 1.1L), which has eight Si-drift detectors in an annular back-scattering configuration positioned around the specimen (Gianoncelli et al., 2009). In LEXRF mode, the selected regions were scanned with 1.7-keV excitation energy with a 5-s dwell time and a 1-μm step size (pixel). The largest area that could be mapped in any given scan was 80 × 80 μm; therefore, multiple individual scans were combined as a mosaic to examine the distribution of Al from the outside of the root through to the inner tissues. Each individual scan took approximately 9 h to complete, with the largest mosaic, which consisted of 26 individual scans, taking approximately 234 h to complete. The LEXRF spectra were fitted using PyMCA (Sole et al., 2007).

NanoSIMS analysis was performed using a CAMECA NanoSIMS 50L with a focused O^- ion beam. The beam was scanned over the surface of the sample, and the sputtered secondary ions were extracted using a double-focusing mass spectrometer. Images were captured with a lateral resolution of approximately 300 nm for areas of 30 × 30 μm, taking approximately 40 min per map. Maps were collected simultaneously for $^{27}Al^+$ and $^{23}Na^+$.

Mechanical Properties of Cell Walls

Resulting from the data of previous experiments, creep experiments were conducted using a DMTA-II (TA Instruments) to establish the effects of Al on cell wall rigidity as found by Jones et al. (2006) with maize (*Zea mays*). Seedlings were grown overnight in basal solution before being exposed to 30 μM Al for 0.5, 1, or 3 h. Roots were clamped in the torsion tool, which was enclosed to limit sample dehydration, with a gauge length of 5 mm starting approximately 3 mm behind the root apex. A constant stress of 15,000 Pa was applied, and the length of the root was monitored over a period of 20 min, with three replicates per treatment. Although examined fresh (Cosgrove, 1993), a preliminary experiment had determined that roots cease to elongate after clamping and crushing the apex (Supplemental Fig. S7). This established that the creep measured after the application of stress was not caused by the continued natural elongation of the fresh roots. Data were analyzed using a grouped regression analysis in GenStat (VSN International) fitting exponential curves.

Roles of Ethylene and Auxin

Soybean seeds were sown in trays of wet grade 2 vermiculite in growth chambers (Percival Scientific) maintained at 28°C during the day (16 h) and 24°C during the night (8 h) with either 70% (day) or 85% (night) relative humidity. *Agrobacterium rhizogenes* strain K599 (Savka et al., 1990) was transformed with the binary vector (plasmid pCAMBIA1301 containing GFP and with the DR5 promoter driving expression of the GUS gene, a gift of Senthil Subramanian) by electroporation and grown at 28°C on Luria-Bertani medium (10 g of tryptone, 5 g of yeast extract, 10 g of NaCl, and 15 g of agar per liter) agar plates containing 30 mg L^{-1} rifampicin and 50 mg L^{-1} kanamycin. Five days after planting, a suspension of transformed *Agrobacterium* sp. and water was used to transform the soybean seedlings using the hypocotyl stabbing method (Kereszt et al., 2007). After 18 d, which ensured sufficient growth of transformed (hairy) roots, the stems were cut at the hypocotyl just below the infection site, and the excised plants were transferred to an 11-L container filled with a complete nutrient solution containing 680 μM NO_3^--N, 120 μM NH_4^+-N, 380 μM Ca, 350 μM S, 305 μM K, 100 μM Na, 97 μM Mg, 50 μM Fe-EDTA, 5 μM P, 3 μM B, 1 μM Mn, 1 μM Zn, 0.5 μM Cu, and 0.02 μM Mo. After 4 d of growth in these nutrient solutions, the plants were transferred to 11-L containers with the same basal composition and one of 24 treatments (three controls and 21 with Al). The controls, all with no added Al, were the binary vector with DR5 elements removed (negative GUS control), a 35S::GUS with the cauliflower mosaic virus 35S promoter constitutively driving the GUS gene (positive GUS control), and a DR5::GUS control. To examine the effects of Al, the DR5::GUS hairy roots were exposed to 10, 30, or 75 μM Al (Supplemental Table S1) each for six exposure periods (0.083 [5 min], 0.25, 0.5, 1.5, 3, and 6 h). The remaining three treatments examined the effects of 30 μM Al with 4 μM AVG for 0.5, 3, or 6 h. Plants were harvested, and the hairy roots were vacuum infiltrated using ice-cold 0.5% (w/v) paraformaldehyde and then rinsed two times in 100 mM NaH_2PO_4 buffer (pH 7.0). After rinsing, the roots were placed in a staining solution [0.1 mM 5-bromo-4-chloro-3-indolyl-β-glucuronic acid, 100 mM NaH_2PO_4 buffer (pH 7.0), 5 mM EDTA, 0.5 mM $K_4Fe(CN)_6$, 0.5 mM $K_3Fe(CN)_6$, and 0.1% (v/v) Triton X-100]. Roots were stained for 24 h in the dark at 37°C and then dehydrated using an ethanol series (10%, 10%, 25%, 50%, and 70% [v/v]).

Al in Root Apical Tissues

The concentration of Al in bulk apical tissues was determined by initially growing 60 soybean seedlings in each of four 22-L containers filled with 1 mM $CaCl_2$ and 5 μM H_3BO_3 at pH 4.8. After the roots were approximately 50 mm in length, the seedlings were moved into treatment solutions containing 1 mM $CaCl_2$, 5 μM H_3BO_3, and 30 μM $AlCl_3$ at pH 4.8. The seedlings were harvested after exposure to the Al for 0, 1.5, 5, or 12 h, with the roots separated into segments 0 to 3 mm and 3 to 10 mm from the apex. The tissues were digested using nitric and perchloric acids before analysis using inductively coupled plasma optical emission spectroscopy.

Supplemental Data

The following supplemental materials are available.

Supplemental Figure S1. Changes in RER after exposure to Al.

Supplemental Figure S2. Profiles of velocity along the elongation zone.

Supplemental Figure S3. Profiles of relative velocity along the elongation zone.

Supplemental Figure S4. Rate of cell expansion along the elongation zone.

Supplemental Figure S5. Effects of Al on the expression of the GUS reporter gene fused to a minimal promoter and the DR5 auxin-responsive promoter element (DR5::GUS).

Supplemental Figure S6. Effects of Al on the expression of GUS fused to a minimal promoter and the auxin-responsive promoter element DR5.

Supplemental Figure S7. Extension of cell walls of fresh soybean roots without Al.

Supplemental Table S1. Toxicity symptoms observed after exposure to Al.

Supplemental Table S2. Bulk concentrations of Al in root apical tissues.

Supplemental Table S3. Speciation of Al in the nutrient solutions.

Supplemental Movie S1. Formation of a radial swelling behind the root apex, showing images captured 270 to 500 min after exposure to 30 μM Al.

Supplemental Movie S2. Formation of ruptures behind the root apex, showing images captured 600 to 880 min after exposure to 75 μM Al.

Received November 5, 2014; accepted February 7, 2015; published February 10, 2015.

LITERATURE CITED

Alarcon MV, Lloret PG, Salguero J (2013) Auxin-ethylene interaction in transversal and longitudinal growth in maize primary root. Botany **91:** 680–685

Baskin TI (2013) Patterns of root growth acclimation: constant processes, changing boundaries. Wiley Interdiscip Rev Dev Biol **2:** 65–73

Basu P, Pal A, Lynch JP, Brown KM (2007) A novel image-analysis technique for kinematic study of growth and curvature. Plant Physiol **145:** 305–316

Blamey FPC, Nishizawa NK, Yoshimura E (2004) Timing, magnitude, and location of initial soluble aluminium injuries to mungbean roots. Soil Sci Plant Nutr **50:** 67–76

Carpita NC, McCann M (2000) The cell wall. *In* BB Buchanan, W Gruissem, RL Jones, eds, Biochemistry and Molecular Biology of Plants. American Society Plant Physiologists, Rockville, MD, pp 52–109

Cosgrove DJ (1993) Wall extensibility: its nature, measurement and relationship to plant cell growth. New Phytol **124:** 1–23

Eswaran H, Reich P, Beinroth F (1997) Global distribution of soils with acidity. *In* AC Moniz, ed, Plant-Soil Interactions at Low pH. Brazilian Soil Science Society, Sao Paulo, Brazil, pp 159–164

Eticha D, Stass A, Horst WJ (2005) Localization of aluminium in the maize root apex: can morin detect cell wall-bound aluminium? J Exp Bot **56:** 1351–1357

Gianoncelli A, Kaulich B, Alberti R, Klatka T, Longoni A, de Marco A, Marcello A, Kiskinova M (2009) Simultaneous soft X-ray transmission and emission microscopy. Nucl Instrum Methods Phys Res A **608:** 195–198

Guillemin F, Guillon F, Bonnin E, Devaux MF, Chevalier T, Knox JP, Liners F, Thibault JF (2005) Distribution of pectic epitopes in cell walls of the sugar beet root. Planta **222:** 355–371

Horst WJ, Wang Y, Eticha D (2010) The role of the root apoplast in aluminium-induced inhibition of root elongation and in aluminium resistance of plants: a review. Ann Bot **106:** 185–197

Jones DL, Blancaflor EB, Kochian LV, Gilroy S (2006) Spatial coordination of aluminium uptake, production of reactive oxygen species, callose production and wall rigidification in maize roots. Plant Cell Environ **29:** 1309–1318

Kaulich B, Bacescu D, Susini J, David C, Di Fabrizio E, Morrison GR, Charalambous P, Thieme J, Wilhein T, Kovac J, et al (2006) TwinMic: A European Twin X-ray Microscopy Station Commissioned at ELETTRA, IPAP Conference Series, Vol 3. Himeji, Japan, pp 22–25

Kereszt A, Li D, Indrasumunar A, Nguyen CD, Nontachaiyapoom S, Kinkema M, Gresshoff PM (2007) *Agrobacterium rhizogenes*-mediated transformation of soybean to study root biology. Nat Protoc **2:** 948–952

Kidd PS, Llugany M, Poschenrieder C, Gunsé B, Barceló J (2001) The role of root exudates in aluminium resistance and silicon-induced amelioration of aluminium toxicity in three varieties of maize (*Zea mays* L.). J Exp Bot **52:** 1339–1352

Kinraide TB (1999) Interactions among Ca^{2+}, Na^{+} and K^{+} in salinity toxicity: quantitative resolution of multiple toxic and ameliorative effects. J Exp Bot **50:** 1495–1505

Kollmeier M, Felle HH, Horst WJ (2000) Genotypical differences in aluminum resistance of maize are expressed in the distal part of the transition zone: Is reduced basipetal auxin flow involved in inhibition of root elongation by aluminum? Plant Physiol **122:** 945–956

Kopittke PM, Blamey FPC, Menzies NW (2008) Toxicities of soluble Al, Cu, and La include ruptures to rhizodermal and root cortical cells of cowpea. Plant Soil **303:** 217–227

Kopittke PM, Menzies NW, Wang P, McKenna BA, Wehr JB, Lombi E, Kinraide TB, Blamey FPC (2014) The rhizotoxicity of metal cations is related to their strength of binding to hard ligands. Environ Toxicol Chem **33:** 268–277

Llugany M, Poschenrieder C, Barceló J (1995) Monitoring of aluminium-induced inhibition of root elongation in four maize cultivars differing in tolerance to aluminium and proton toxicity. Physiol Plant **93:** 265–271

Ma JF, Shen R, Nagao S, Tanimoto E (2004) Aluminum targets elongating cells by reducing cell wall extensibility in wheat roots. Plant Cell Physiol **45:** 583–589

Menzies NW, Bell LC, Edwards DG (1994) Exchange and solution-phase chemistry of acid, highly weathered soils. I. Characteristics of soils and the effects of lime and gypsum amendments. Aust J Soil Res **32:** 251–267

Parker DR (1995) Root growth analysis: an underutilised approach to understanding aluminium rhizotoxicity. Plant Soil **171:** 151–157

Pierik R, Verkerke W, Voesenek RACJ, Blom KWPM, Visser EJW (1999) Thick root syndrome in cucumber (*Cucumis sativus* L.): a description of the phenomenon and an investigation of the role of ethylene. Ann Bot **84:** 755–762

Rangel AF, Rao IM, Horst WJ (2009) Intracellular distribution and binding state of aluminum in root apices of two common bean (*Phaseolus vulgaris*) genotypes in relation to Al toxicity. Physiol Plant **135:** 162–173

Rengel Z (1997) Mechanisms of plant resistance to toxicity of aluminium and heavy metals. *In* AS Basra, RK Basra, eds, Mechanisms of Environmental Stress Resistance in Plants. Harwood Academic, Amsterdam, pp 241–276

Sasaki M, Yamamoto Y, Ma JF, Matsumoto H (1997) Early events induced by aluminum stress in elongating cells of wheat root. Soil Sci Plant Nutr **43:** 1009–1014

Savka M, Ravillion B, Noel G, Farrand S (1990) Induction of hairy roots on cultivated soybean genotypes and their use to propagate the soybean cyst nematode. Phytopathology **80:** 503–508

Silk WK (1992) Steady form from changing cells. Int J Plant Sci **153:** S49–S58

Sole VA, Papillon E, Cotte M, Walter P, Susini J (2007) A multiplatform code for the analysis of energy-dispersive X-ray fluorescence spectra. Spectrochim Acta Part B At Spectrosc **62:** 63–68

Sun P, Tian QY, Chen J, Zhang WH (2010) Aluminium-induced inhibition of root elongation in *Arabidopsis* is mediated by ethylene and auxin. J Exp Bot **61:** 347–356

Swarup R, Perry P, Hagenbeek D, Van Der Straeten D, Beemster GT, Sandberg G, Bhalerao R, Ljung K, Bennett MJ (2007) Ethylene upregulates auxin biosynthesis in *Arabidopsis* seedlings to enhance inhibition of root cell elongation. Plant Cell **19:** 2186–2196

Turner M, Nizampatnam NR, Baron M, Coppin S, Damodaran S, Adhikari S, Arunachalam SP, Yu O, Subramanian S (2013) Ectopic expression of miR160 results in auxin hypersensitivity, cytokinin hyposensitivity, and inhibition of symbiotic nodule development in soybean. Plant Physiol **162:** 2042–2055

Winship LJ, Obermeyer G, Geitmann A, Hepler PK (2010) Under pressure, cell walls set the pace. Trends Plant Sci **15:** 363–369

Yamamoto Y, Kobayashi Y, Matsumoto H (2001) Lipid peroxidation is an early symptom triggered by aluminum, but not the primary cause of elongation inhibition in pea roots. Plant Physiol **125:** 199–208

Zelinová V, Halušková L, Huttová J, Illéš P, Mistrík I, Valentovičová K, Tamás L (2011) Short-term aluminium-induced changes in barley root tips. Protoplasma **248:** 523–530